Ferroelectric properties of epitaxial $BaTiO_3$ thin films and heterostructures on different substrates

O. Trithaveesak, J. Schubert,[a] and Ch. Buchal

Institut für Schichten und Grenzflächen (ISG1-IT) and Center for Nanoelectronic Systems in Information Technology (CNI), Forschungszentrum Jülich GmbH, D-52425 Jülich, Germany

(Received 29 March 2005; accepted 12 October 2005; published online 2 December 2005)

Ferroelectric thin films of $BaTiO_3$ and $BaTiO_3/SrRuO_3$ epitaxial heterostructures on different single-crystalline substrates were fabricated by pulsed laser deposition. The $BaTiO_3$ films of 100–400 nm thickness show high structural perfection and *c*-axis-oriented growth. For the electrical characterization of the $BaTiO_3$ in a thin-film capacitor structure, Pt top electrodes were deposited by *e*-beam evaporation. The results are compared to the current experimental and theoretical models. Special consideration is given to the model of charge injection from the electrodes. © *2005 American Institute of Physics*. [DOI: 10.1063/1.2135891]

I. INTRODUCTION

In bulk form, $BaTiO_3$ (BTO) is a very carefully studied ferroelectric crystal. It has been widely used as a model system for the explanation of ferroelectric phenomena.[1–3] A number of papers have discussed thin films of BTO as well.[4–7] Recently epitaxial BTO films have been prepared on different single-crystalline oxide substrates by pulsed laser deposition (PLD).[8–12] Such epitaxial films show an excellent structural perfection, which is comparable to that of BTO single crystals. They provide useful optical and electro-optical properties, which have been employed for the fabrication of integrated optical devices.[11,13]

For these optical devices, the necessary film thickness is approximately 1 μm. For micro- and nanoelectronics, much thinner films are of interest. Very impressive data of the ferroelectric properties of ultrathin $BaTiO_3$ films of 3–30 nm thickness have been obtained recently by Ref. 12. However, the properties of nanoscale films may deviate strongly from the bulk crystalline values, even for epitaxial films. One reason is the strain and stress within the thin BTO films, arising from the interfaces. This problem has been studied theoretically by Refs. 14 and 15. Of outmost importance is the modification of the ferroelectric response due to the interface boundary conditions and the film thickness (size effect). One observation is a pronounced increase of the coercive field E_c for decreasing film thickness.[2,3,16,17] This effect has been observed even for polycrystalline ferroelectric lead zirconate titanate (PZT) thin-film capacitors.[18] The understanding and the control of size effects is essential for the implementation of ferroelectrics into microelectronic devices.[12,19] In this study we investigated the ferroelectric properties of BTO films with a thickness from 100 to 400 nm, grown on the following substrates: $SrTiO_3(100)$, $YAlO_3(100)$, $LaAlO_3(100)$, $MgO(100)$, $NdGaO_3(110)$, and $DyScO_3(110)$. The samples were prepared either with a conductive intermediate layer of $SrRuO_3$ or directly on the insulating substrates.

The sample preparation and the methods of characterization are described in Sec. II. The experimental results will be presented in Sec. III. Subsequently the discussion is given in Sec. IV.

II. EXPERIMENTAL PROCEDURE

Starting from different single crystals as substrates, PLD with a KrF excimer laser (wavelength 248 nm, pulse length 20 ns, fluence 2.5 J/cm^2) was used to grow an epitaxial $SrRuO_3$ (SRO) bottom electrode and on top of this electrode the epitaxial BTO film. The SRO films were grown at a substrate temperature of ~600 °C and an oxygen gas pressure of 0.5 mbar within the chamber. These are similar growth conditions as used by other authors.[13,20] The BTO films were prepared at a substrate temperature of ~700 °C and a chamber pressure of 0.002 mbar.[8] A subsequent annealing step in an oxygen atmosphere at 800 °C was performed for several sets of samples but did not change the measured electrical parameters. The film thickness was either controlled directly by the deposition time or by starting from a BTO film of 300 nm thickness and a subsequent Ar ion-beam etching process to locally reduce the film thickness. A sample with four different thickness steps is shown in Fig. 1. This second approach ensures that several sets of BTO samples of different film thicknesses and identical interfaces to the bottom electrode are fabricated.

In order to fabricate a set of nanoscale capacitors of different areas, a 150 nm layer of Pt metal was deposited by electron-beam evaporation and subsequently patterned by Ar ion etching to define the top electrodes of 0.01–0.1 mm^2 area. These are schematically depicted in Fig. 1 as well. Care was taken that the samples were not subject to elevated temperatures. The ferroelectric hysteresis loops were evaluated with the FE module of the aixACCT thin-film TF2000 analyzer. In addition to the measurement with a continuous triangle signal (dynamic method) the stepwise measurement technique (quasistatic method) was used to record the static hysteresis *P-V* loops. The detailed description of this technique has been given in Ref. 21. In addition, we used a HP4292A impedance analyzer to measure the capacitance as

[a]Author to whom correspondence should be addressed; electronic mail: j.schubert@fz-juelich.de

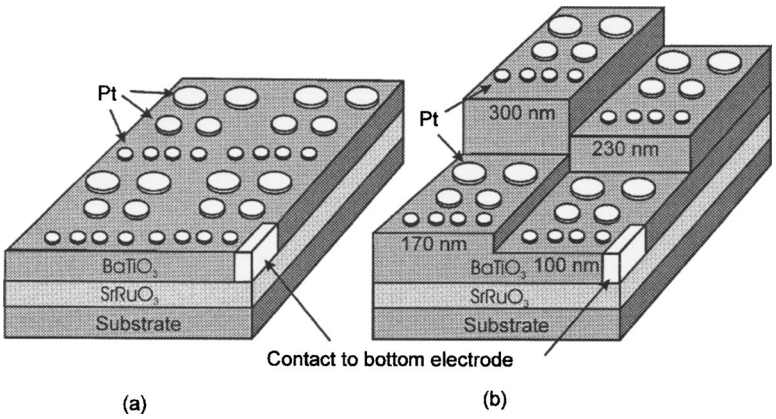

FIG. 1. Schematic of the two different ways to prepare the samples: (a) Several $BaTiO_3$ films of different thicknesses were grown. Then Pt electrodes were deposited. (b) One $BaTiO_3$ film of 300 nm thickness was prepared and locally etched. Subsequently electrodes were deposited onto the different steps.

a function of temperature and bias voltage. All electrical measurements were taken at temperatures ranging from room temperature down to −196 °C (77 K).

III. RESULTS

A. Structural characterization

Figure 2 shows the Rutherford backscattering/channeling (RBS/C) spectra of the BTO/SRO heterostructure on a single-crystal $SrTiO_3$ (STO) substrate. A 1:1 Ba:Ti ratio and a $BaTiO_3$ film thickness of 300 nm are verified from the spectrum taken in a "random" direction. The aligned spectrum ("channeling") shows a strong decrease of the signal, if compared to the random spectrum. The minimum yield χ_{min} is 3%, which demonstrates high crystalline quality of the BTO film. This minimum yield χ_{min} is typical for all investigated films and all thickness values. It is equivalent to RBS/C results from BTO single crystals.

In addition to RBS/C, x-ray-diffraction (XRD) measurements were performed. In Table I the results from the epitaxial films with a thickness from 100 to 400 nm are summarized. A thickness variation of the lattice parameters was not observed. All BTO films showed *c*-axis orientation growth (the long axis perpendicular to the plane of the substrates). Compared to bulk crystalline BTO, the measured out-of-plane axis (*c* axis) is significantly larger. The in-plane axis (*a* axis) does not significantly differ from the corresponding bulk value. Table II shows structural results of $BaTiO_3/SrRuO_3$ heterostructures grown on different substrates. In all cases, the $BaTiO_3$ films are strained and show an elongated *c* axis. The low O_2 pressure of 0.002 mbar was optimized for optical transparency but may result in oxygen vacancies, which lead to a lattice expansion of the $BaTiO_3$. Tables III and IV give the results for thin epitaxial $SrRuO_3$ films on different substrates. These films have been used as electrodes for the electrical measurements.

B. Electrical characterization

1. Polarization and residual conductivity

a. Measurements at ambient temperature The polarization, the corresponding displacement, and the leakage currents were recorded as a function of applied voltage using the aixACCT TF2000 analyzer. Figure 3(a) shows the results from a capacitor structure with a 300 nm BTO film. For all

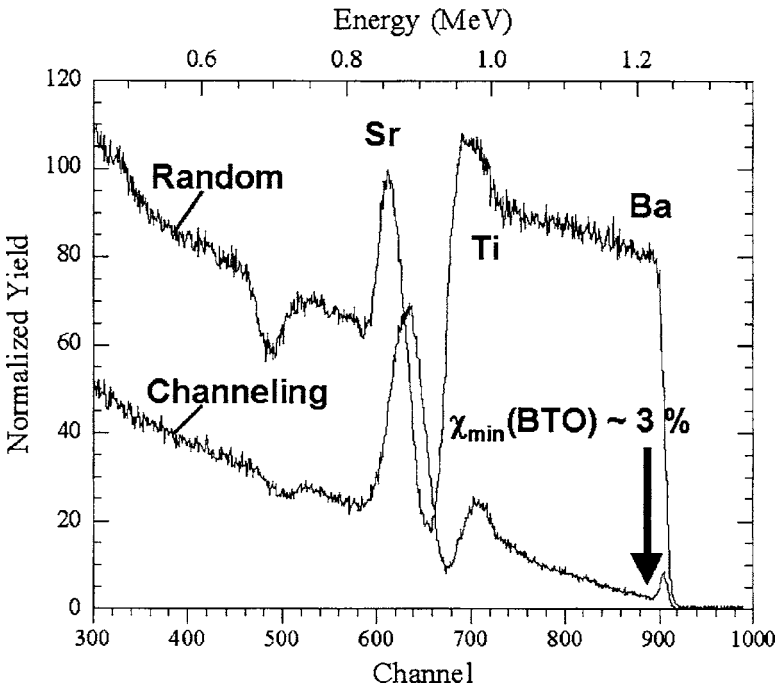

FIG. 2. RBS and channeling spectra of a 300 nm $BaTiO_3$/60 nm $SrRuO_3$ heterostructure grown onto a $SrTiO_3$(100) substrate.

TABLE I. Crystallographic data of the materials used.

	c axis (Å)	a axis (Å)	FWHM (°)
$BaTiO_3$ epitaxial films	4.10±0.02	4.00±0.03	0.40±0.05
$BaTiO_3$ single crystal	4.03	3.99	
$SrRuO_3$ epitaxial films	3.98±0.02	3.90±0.03	0.07±0.05
$SrTiO_3$ substrate	3.90	3.90	

samples shown in Fig. 3, the capacitor area was 0.1 mm^2 and the measuring frequency 10 kHz. The peaks of the *I-V* loop are typical for a ferroelectric capacitor. They indicate the switching of the polarization. If the film thickness is reduced from 300 to 230 nm [Fig. 3(b)], small additional leakage currents are observed at high negative voltages. Yet, the switching peaks still are recognized. The asymmetry of the *I-V* curves grows excessively in the capacitor with a 100 nm film [Fig. 3(c)]. In this case any switching process is obscured by the leakage current. A similar asymmetric current characteristic was observed in $BaTiO_3/La_2CuO_4$ heterostructures with Pt electrodes by Okano *et al.*[22] They argue that the diodelike behavior depends on the conductive oxide electrode. For a *p*-type conductor as La_2CuO_4 this characteristic will be seen if a high negative voltage is applied to the Pt electrode. The results from our heterostructure confirm that $SrRuO_3$ is a *p*-type conductor, as expected.[23]

b. Measurements at lower temperatures Lowering the temperature leads to a strong reduction of the conductivity. This corroborates the hypothesis that the observed leakage currents are due to thermally activated processes. During *I-V* measurements at −100 °C the leakage currents in the thinner films are still noticeable, but at −150 °C the situation is remarkably improved. A typical set of 10 kHz hysteresis loops of capacitors of different thicknesses is displayed in Fig. 4. These loops show that the coercive field and the spontaneous polarization increase for thinner films. This is in agreement with the observations of Ref. 12 on ultrathin films.

At a temperature of −196 °C the leakage currents are sufficiently small to permit a polarization measurement by a quasistatic method. In Figs. 5(a) and 5(b) the polarization of as-grown samples and of a thinned sample (by the Ar etching process) are plotted as a function of the applied voltage. Equivalent to the 10 kHz dynamic loops at $T=-150$ °C (Fig. 4), an influence of the film thickness is observed. These data have been taken in a static mode with hold times exceeding several seconds. Therefore a ferroelectric relaxation is excluded. Moreover, the coercive voltage V_c of the films is found to be independent of the film thickness. Even the sets of the most uniform samples, made by etching, show a negligibly small variation of V_c for all thickness values. These results are summarized in Fig. 6; the average spontaneous polarization $[(P_{s+}+|P_{s-}|)/2]$ and the coercive voltage $[(V_{c+}+|V_{c-}|)/2]$ are plotted as a function of film thickness.

2. Capacitance

a. C-V measurements The dielectric response ε_r of ferroelectric films at varying bias voltage, the "*C-V* curve," has a butterflylike form, see Fig. 7. The dielectric constant ε_r has been calculated using the parallel-plate capacitor equation. These data have been measured at a temperature of −196 °C, using the etched sample. A comparison between the dynamic polarization, the static polarization loop, and the *C-V* curves shows that the peaks of the *C-V* curves are located, as expected, at the coercive voltage of the quasistatic loop. Clearly ΔE_C increases and ε_r drops for thinner films. The observed decrease of ε_r is consistent with the existence of a thin passive interfacial layer of reduced dielectric response.[3,18,23–25]

b. Temperature dependence of the small signal dielectric response We have measured the temperature dependence of the dielectric constant (capacitance) and the electrical loss ($\tan\delta$) at zero bias during a very slow temperature ramp from $T=-196$ °C up to ambient temperature. These measurements were performed at a frequency of 1 and 10 kHz with a small excitation signal of 70 mV_{eff}, without applying any dc bias and without ramping through the hysteresis loop. The dielectric constant ε_r was determined using the parallel-plate capacitor equation. Figure 8(a) demonstrates a continuous decrease of ε_r with falling temperature. The data at lower frequency show a higher value of ε_r. A similar observation was made on sol-gel-processed polycrystalline BTO thin films.[26] These findings are consistent with a thermally activated domain-wall mobility, which leads to a reduced dielectric response at lower temperatures.

The plot of the dielectric loss ($\tan\delta$) as a function of temperature [Fig. 8(b)] shows a pronounced maximum, which is strongly depending on the frequency. A similar behavior of $\tan\delta$ is seen for STO/SRO heteroepitaxial capacitors.[27] In a further analysis we calculated the normalized ac conductance G/ω from the product of $\tan\delta$ and the capacitance. The results are plotted as functions of the temperature in Fig. 8(c). The G/ω peaks are strongly resembling the frequency dependence of a thermally activated conductivity in the presence of deep-level traps, as seen in semiconductors as well.[28]

TABLE II. Structural properties of the BTO layers grown on different substrates. Given are the lattice parameters of the tetragonal unit cell, the full width at half maximum (FWHM) $\Delta\omega$ of the BTO (002) reflex, the minimum yield χ_{min} at the Ba signal, and the lattice mismatch u_m between BTO and the substrate.

Substrate	d(BTO) (nm)	c axis (Å)	a axis (Å)	$\Delta\omega$ (°)	χ_{min} (%)	u_m (%)
$SrTiO_3$	100–400	4.10±0.02	4.00±0.02	0.4±0.05	3	−2.56
$YAlO_3$	210	4.07	4.00	0.56	3.5	−9
$LaAlO_3$	170	4.06	3.95	0.44	3	−5.3
MgO	170	4.07	4.02	0.5	3	5.1
$NdGaO_3$	190	4.08	4.00	0.5	6	−3.4
$DyScO_3$	210	4.14	3.97	0.35	3	−1.5

TABLE III. Structural properties of the SRO layers grown on different substrates. Given are the lattice parameters of the SRO unit cell, the FWHM $\Delta\omega$ of the SRO (002) reflex, the minimum yield χ_{min} at the Ru signal, and the lattice mismatch u_m between SRO and the substrate.

Substrate	c axis (Å)	a axis (Å)	$\Delta\omega$ (°)	χ_{min} (%)	u_m (%)
$SrTiO_3$	3.98±0.02	3.90±0.02	0.07±0.05	2	0.7
$YAlO_3$	3.94	3.94	1.00	6	−7.4
$LaAlO_3$	3.96	3.87	0.50	10	−3.7
MgO	3.93	···	1.2	20	6.65
$NdGaO_3$	3.96	3.87	0.5	16	−1.8
$DyScO_3$	3.96	3.91	0.07	6	≈0

IV. DISCUSSION

The dielectric response of nanoscale ferroelectric films or capacitors is influenced by many different factors, which frequently cannot be singled out. As a consequence, the available literature does not yet provide a consistent explanation of the published observations, and controversial models are under discussion. All ferroelectric films are sensitive to strain and stress, to dislocations and point defects, and to the grain structure.[1–3,14,29–31] Polycrystalline layers have the strongest technological relevance, but their ferroelectric response differs from that of single-crystalline material.[1,31] In our previous experiments, the overall quality of the BTO films had been optimized for the highest optical transparency, i.e., for lowest propagation losses of guided light in integrated optics modulators.[9] The crystalline perfection of the BTO is well demonstrated. We do not see any in-plane strain. Nevertheless, all films show a definite (approximately 2%) out-of-plane elongation of the BTO c axis, if compared to the bulk values, see Tables I and II. A possible explanation is a small concentration of negatively charged vacancies at oxygen lattice positions. If investigated by atomic force microscopy (AFM) in the piezoresponse mode, the BTO films show one single ferroelectric orientation (out of plane) without any domain structure.[32] This measurement demonstrates a strong electrostatic interaction at the interface between the ferroelectric BTO unit cells and the underlying SRO/STO. In addition, the observation of a single domain structure has direct implications for the polarization reversal dynamics of the thin films. Conventional theories consider the nucleation and wall dynamics of domains to describe the switching process and the thickness dependence of the coercive field.[2,33–35] It is well established that thin films have much higher coercive fields than expected from the bulk data. For example, bulk BTO single crystals have a coercive field E_c of approximately 1 kV/cm,[1] but our data show values of up to 300 kV/cm for the thinnest films. This observation is in complete agreement with results of Refs. 12 and 19. It also scales with data for ultrathin $PbZrTiO_3$ films, which show an

TABLE IV. Thickness and resistivity of SRO films grown on different substrates.

Substrate	Thickness (nm)	$\rho(T=250\ \text{K})$ ($\mu\Omega$ cm)
$SrTiO_3$	140	390
$NdGaO_3$	130	450
$YAlO_3$	50	610

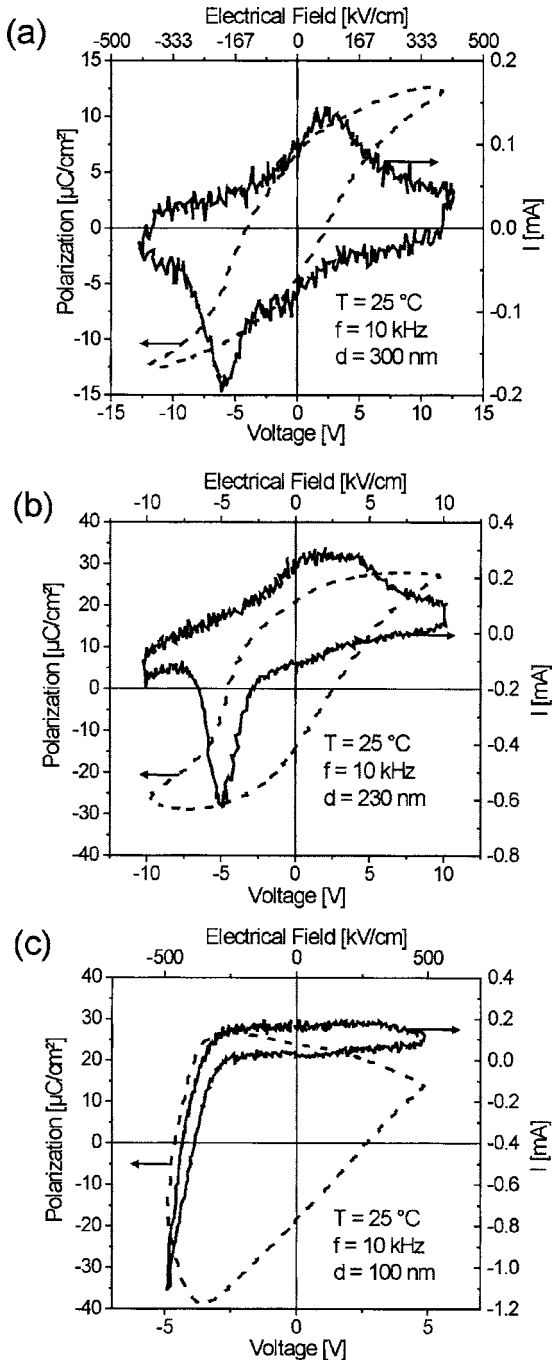

FIG. 3. Hysteresis loops and corresponding current (I-V) loops of a capacitor with (a) 300 nm, (b) 230 nm, and (c) 100 nm $BaTiO_3$ film thickness, measured at room temperature.

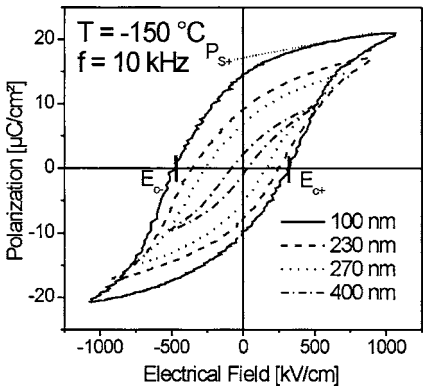

FIG. 4. Hysteresis loops at $T=-150\ ^{\circ}\mathrm{C}$, measured by the dynamic method ($f=10$ kHz).

increase of E_c up to 1.2 MV/cm for an 8 nm film.[19] These numbers reach or even exceed the high values from theoretical estimates of E_c by the Landau-Devonshire theory, which assumes a polarization reversal *without* the formation of domains.

A very important issue is the available carrier density within the electrodes in contact with the ferroelectric.[36,37] We have chosen SRO, which provides up to 2×10^{22} carriers/cm^3 on the bottom side and metallic Pt as the top electrode.[23] This arrangement is intended to form an ideal capacitor sandwich, because these electrodes should be able to compensate the BTO polarization surface charge of 25 μC/cm^2 on a length scale of 0.1 nm, resulting in a zero

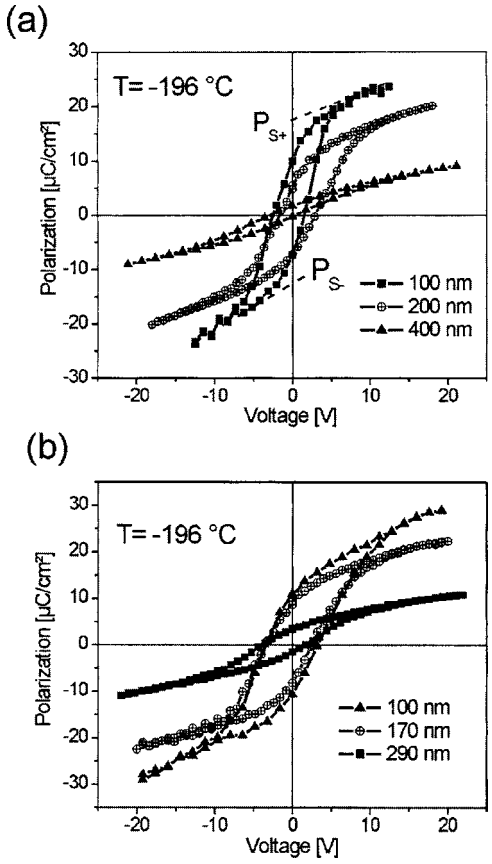

FIG. 5. Static polarization loops as a function of the voltage at $T=-196\ ^{\circ}\mathrm{C}$ for (a) three as-grown films of different thicknesses, and (b) three different capacitors, made by etching steps into one film

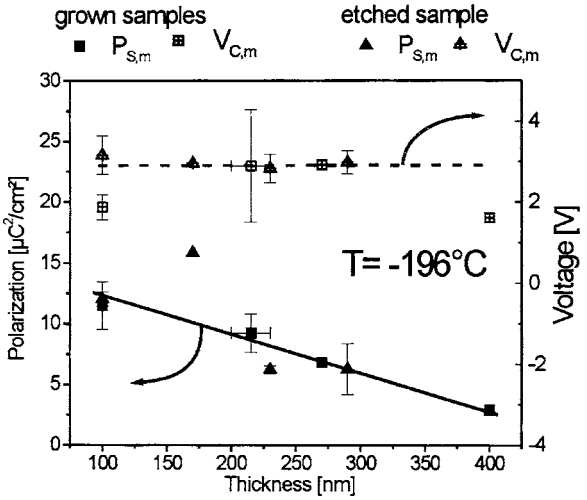

FIG. 6. Thickness dependence of the average spontaneous polarization and coercive voltage, measured at the static hysteresis loops of the as-grown films and etched films, recorded at $T=-196\ ^{\circ}\mathrm{C}$.

depolarization field within the BTO. Nevertheless, our observation of a constant coercive voltage V_c of approximately 3 V for all the films must be due to a different effect.

The thickness dependence of ε_r, as shown in Fig. 6, hints towards the existence of an intermediate, insulating, nonferroelectric interfacial layer, as has been discussed by many authors.[2,3,16,23–25,38] It may be assumed, that this layer even consists of good BTO, which is unable to switch due to strong electrostatic interactions with the substrate. A crucial mechanism is the injection of charges through this insulating layer towards the internal interface to the switchable ferroelectric. If this layer indeed is identical for all films investigated (see Fig. 1), a constant breakthrough voltage is expected and determines the onset of polarization reversal. Assuming a breakthrough field of 3 MV/cm hints towards a passive layer thickness of 5–10 nm. At the hypothetical interface between the passive layer and the BTO the injected charge has to be stored and removed again during one complete cycle of a hysteresis loop. We note that the available density of states to store the displacement current at the internal interface within the crystal between the passive and the active part of the BTO is significant.

Finally we turn our attention to the measured polariza-

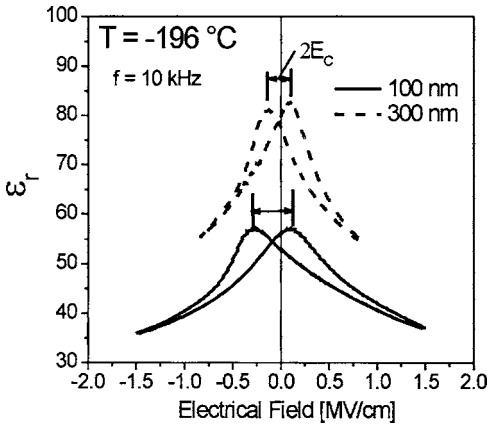

FIG. 7. *C-V* curves of a capacitor, using an etched sample with 300 and 100 nm $BaTiO_3$ films, measured $T=-196\ ^{\circ}\mathrm{C}$.

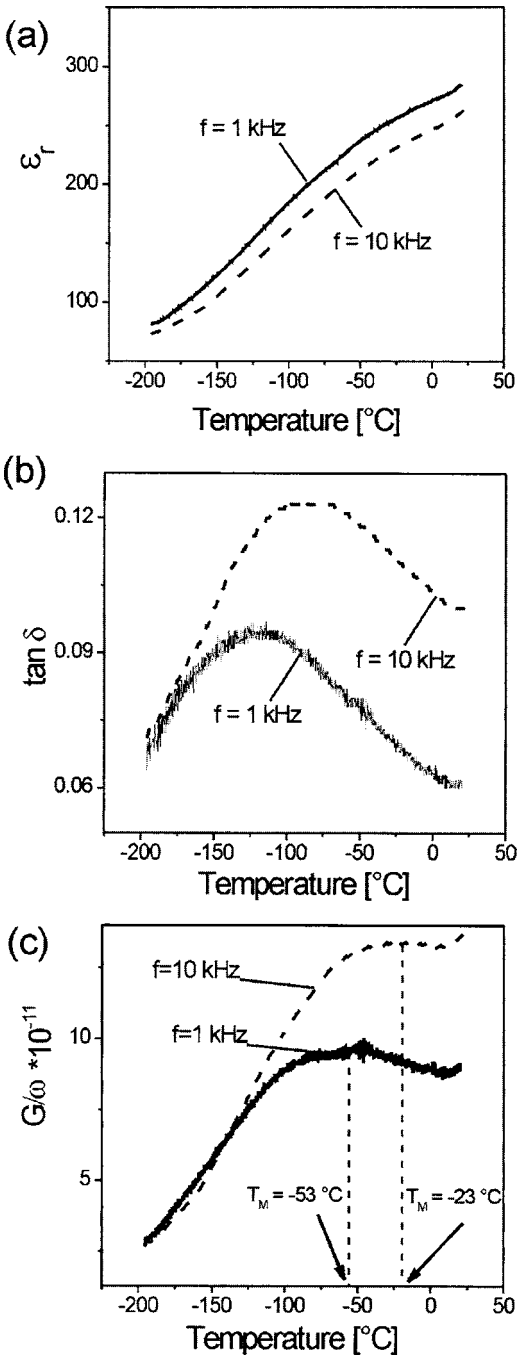

FIG. 8. Temperature dependence of (a) ε_r, (b) $\tan\delta$, and (c) normalized conductance G/ω, measured without bias voltage at $f=1$ and 10 kHz.

tion P_s (Figs. 4 and 6). For the thinnest film, P_s nearly reaches the value expected from the bulk data, but for the thicker films, a continuously lower value for P_s is measured. A recent publication carefully discusses the possibility to stabilize or even enhance P_s at the interface to the substrate due to the epitaxy.[39]

V. CONCLUSION

Nanoscale ferroelectric capacitors are strongly influenced by the interaction with the interfaces to the electrodes due to the epitaxial relations, strain, stress, and Coulomb interactions, even if the ferroelectric material is not degraded by interdiffusion during growth. As a consequence, the polarization of the first few nanometers may be blocked, resulting in a pyroelectric interface layer. Even for nanometer films, the polarization switching of the ferroelectric involves high displacement currents and the same surface charge density as observed for bulk material. The compensating charge has to be provided by high-conductivity electrodes on a subnanometer length scale. The conventional understanding of the domain dynamics does not apply, and very high coercive fields are observed.

We gratefully acknowledge the support from the Deutsche Forschungsgemeinschaft (Grant No. Bu 1258) and from the Graduiertenkolleg "Azentrische Kristalle," Universität zu Köln, as well as PFM results by F. Schlaphof and L. Eng and many helpful discussions with H. H. Kohlstedt.

[1] A. J. Moulson and J. M. Herbert, *Electroceramics* (Chapman and Hall, London, 1997).
[2] J. F. Scott, *Ferroelectric Memories* (Springer, Berlin, 2000).
[3] R. Waser, *Nanoelectronics and Information Technology* (Wiley-VCH, Weinheim, 2003).
[4] K. Abe, S. Komatsu, N. Yanase, K. Sano, and T. Kawakubo, Jpn. J. Appl. Phys., Part 1 **36**, 5846 (1997).
[5] N. Yanase, K. Abe, N. Fukushima, and T. Kawakubo, Jpn. J. Appl. Phys., Part 1 **38**, 5305 (1999).
[6] K. Abe, N. Yanase, and T. Kawakubo, Jpn. J. Appl. Phys., Part 1 **40**, 2367 (2001).
[7] Yu. A. Boikov and T. Claeson, J. Appl. Phys. **89**, 5053 (2001).
[8] L. Beckers, J. Schubert, W. Zander, J. Ziesmann, A. Eckau, P. Leinenbach, and Ch. Buchal, J. Appl. Phys. **83**, 3305 (1998).
[9] A. Petraru, J. Schubert, M. Schmid, and Ch. Buchal, Appl. Phys. Lett. **81**, 1375 (2002).
[10] J. Schubert, O. Trithaveesak, A. Petraru, C. L. Jia, R. Uecker, P. Reiche, and D. G. Schlom, Appl. Phys. Lett. **82**, 3460 (2003).
[11] A. Petraru, J. Schubert, M. Schmid, O. Trithaveesak, and Ch. Buchal, Opt. Lett. **28**, 2527 (2003).
[12] Y. S. Kim *et al.*, Appl. Phys. Lett. **86**, 102907 (2005).
[13] J. Choi, C. B. Eom, G. Rijnders, H. Rogalla, and D. H. A. Blank, Appl. Phys. Lett. **79**, 1447 (2001).
[14] N. A. Pertsev, A. G. Zembilgotov, and A. K. Tagantsev, Phys. Rev. Lett. **80**, 1988 (1998).
[15] A. G. Zembilgotov, N. A. Pertsev, H. Kohlstedt, and R. Waser, J. Appl. Phys. **91**, 2247 (2002).
[16] J. F. M. Cillessen, M. W. J. Prins, and R. M. Wolf, J. Appl. Phys. **81**, 2777 (1997).
[17] N. A. Pertsev, J. R. Contreras, V. G. Kukhar, B. Hermanns, H. Kohlstedt, and R. Waser, Appl. Phys. Lett. **83**, 3356 (2003).
[18] P. K. Larsen, G. J. M. Dormans, D. J. Taylor, and P. J. van Veldhoven, J. Appl. Phys. **76**, 2405 (1994).
[19] J. Rodriguez Contreras, J. Schubert, U. Poppe, O. Trithaveesak, K. Szot, Ch. Buchal, H. Kohlstedt, and R. Waser, Mater. Res. Soc. Symp. Proc. **688**, C8.10 (2002).
[20] C. L. Chen *et al.*, Appl. Phys. Lett. **71**, 1047 (1997).
[21] R. Waser and O. Lohse, Integr. Ferroelectr. **21**, 27 (1998).
[22] M. Okano, D. Sawamura, and Y. Watanabe, Jpn. J. Appl. Phys., Part 1 **37**, 5101 (1998).
[23] S. C. Gausepohl, M. Lee, R. A. Rao, and C. B. Eom, Phys. Rev. B **54**, 8996 (1996).
[24] A. K. Tagantsev and A. Stolichnov, Appl. Phys. Lett. **74**, 1326 (1999).
[25] M. Grossmann, O. Lohse, D. Bolten, U. Boettger, T. Schneller, and R. Waser, J. Appl. Phys. **92**, 2680 (2002).
[26] R. Thomas, V. K. Varadan, S. Komarneni, and D. C. Dube, J. Appl. Phys. **90**, 1480 (2001).
[27] A. Chen, L. E. Cross, Yu. Zhi, G. Ruyan, A. S. Bhalla, and H. H. Jian, Appl. Phys. Lett. **78**, 2754 (2001).
[28] G. Vincent, D. Bois, and P. Pinard, J. Appl. Phys. **46**, 5173 (1975).
[29] N. A. Pertsev, A. K. Tagantsev, and N. Setter, Phys. Rev. B **61**, R825 (2000).
[30] S. P. Alpay, I. B. Misirlioglu, V. Nagarajan, and R. Ramesh, Appl. Phys. Lett. **85**, 2044 (2004).
[31] R. Waser and S. Hoffmann, J. Korean Phys. Soc. **32**, 1340 (1988).

[32]O. Trithaveesak, Thesis, Aachen, 2004, http://darwin.bth.rwth-aachen.de/opus/volltexte/2004/999/.
[33]H. F. Kay and J. W. Dunn, Philos. Mag. **7**, 2027 (1962).
[34]W. J. Merz, Phys. Rev. **95**, 690 (1954).
[35]J. Li, B. Nagaraj, H. Liang, W. Cao, C. H. Lee, and R. Ramesh, Appl. Phys. Lett. **84**, 1174 (2004).
[36]P. Wurfel and I. P. Batra, Phys. Rev. B **8**, 5126 (1973).
[37]D. D. Fong, G. B. Stephenson, S. K. Streiffer, J. A. Eastman, O. Auciello, P. H. Fuoss, and C. Thompson, Science **304**, 1650–1653 (2004).
[38]M. Grossmann, O. Lohse, D. Bolten, U. Boettger, T. Schneller, and R. Waser, J. Appl. Phys. **92**, 2688 (2002).
[39]J. B. Neaton and K. M. Rabe, Appl. Phys. Lett. **82**, 1586 (2003).